Final report on:
Experiments and appraisal to investigate the effect of CO_2/water volume combined with gravity flow characteristics in the Delft area sand reservoirs. Surface & subsurface integration.

Prepared by:	K-H. Wolf, H.M. Nick, H. Salimi
Reviewed by:	K-H. Wolf (TU Delft)
Approved by:	J.Brouwer (CATO-2 Director)

This document contains proprietary information of CATO 2 Program. All rights reserved

Copying of (parts) of this document is prohibited without prior permission in writing

1 Executive Summary (restricted)

Cold mixed CO_2-water injection into geothermal reservoirs can be used for simultaneous geothermal-energy (heat) production and subsurface CO_2 storage. In order to explore the feasibility of the CO_2 combined with geothermal fluid in the Delft area sand reservoirs several studies are conducted. An accurate characterization of the geothermal reservoir is accomplished. Several research questions associated with the geothermal wells including: two-phase flow, mineral scaling, and composite material for casing, are addressed. It is also essential to study the consequence of the CO_2-water injection into geothermal reservoir on the reservoir performance. To achieve this, different research studies are performed: developing a novel two-phase flow numerical approach; incorporating capillary pressure and gravity, studying the effects of dissolved gas on subsurface flow for heat production, as well as optimization of geothermal well doublet placement.

Several models are developed, including a homogeneous reservoir, a layered reservoir, and a heterogeneous reservoir represented by a stochastic-random field. We give a set of simulations for a variety of CO_2-injection concentrations. Different systems of equations apply for single-phase and for two-phase regions. We develop a solution approach, called the non-isothermal negative saturation (NegSat) solution approach, to solve efficiently non-isothermal compositional flow problems (e.g., CO_2-water injection into geothermal reservoirs) that involve phase disappearance, phase appearance, and phase transition. The advantage of the solution approach is that it circumvents using different equations for single-phase and two-phase regions and the ensuing unstable switching procedure. In the NegSat approach, a single-phase multi-component fluid is replaced by an equivalent fictitious two-phase fluid with specific properties. The equivalent properties are such that in the single-phase aqueous region, the extended saturation of a fictitious gas is negative.

We discuss the salient features of the simulations in detail. When two phases are present at the injection side, heterogeneity and layering lead to more CO_2 storage compared to the homogeneous case because of trapping. In addition, layering avoids movement of the CO_2 to the upper part of the reservoir and hence reduces the risk of leakage. Our results also show that heterogeneity and layering change the character of the solution in terms of useful-energy production and CO_2 storage. The simulations can be used to construct a plot of the recuperated useful energy versus maximally stored CO_2. Increasing the amount of CO_2 in the injection mixture leads to bifurcation points at which the character of the solution in terms of energy production and CO_2 storage changes. For overall injected CO_2 mole fractions less than 0.04, the result with gravity is the same as the result without gravity. For larger overall injected CO_2 mole fractions, however, the plot without gravity differs from the plot with gravity due to early breakthrough of a supercritical-CO_2 tongue near the cap rock. The plot of the useful energy (exergy) versus the CO_2 storage capacity in the presence of gravity shows a *Z*-shape. The top horizontal part represents a branch of high exergy recovery and a relatively lower storage capacity, whereas the bottom part represents a branch of lower exergy recovery and a higher storage capacity.

Distribution List

(this section shows the initial distribution list)

External	copies	Internal	Copies

Document Change Record

(this section shows the historical versions, with a short description of the updates)

Version	Nr of pages	Short description of change	Pages

Table of Content

2 Applicable/Reference documents and Abbreviations

2.1 Applicable Documents

(Applicable Documents, including their version, are the "legal" basis to the work performed)

	Title	Doc nr	Version
AD-01d	Toezegging CATO-2b	FES10036GXDU	2010.08.05
AD-01f	Besluit wijziging project CATO2b	FES1003AQ1FU	2010.09.21
AD-02a	Consortium Agreement	CATO-2-CA	2009.09.07
AD-02b	CATO-2 Consortium Agreement	CATO-2-CA	2010.09.09
AD-03g	Program Plan 2013b	CATO2-WP0.A-D03	2013.04.01

2.2 Reference Documents (RD)

(Reference Documents are referred to in the document)

	Title	Nr.	Version
RD-01	Hamidreza Salimi, Karl–Heinz Wolf, and Johannes Bruining. Negative-Saturation Approach for Compositional Flow Simulations of Mixed CO_2–Water Injection into Geothermal Reservoirs Including Phase Appearance and Disappearance. SPE Journal 17(2), 2012.		
RD-02	Hamidreza Salimi and Karl–Heinz Wolf. Integration of Heat–Energy Recovery and Carbon Sequestration. International J. of Greenhouse Gas Control **6**, 2012.		
RD-03	Hamidreza Salimi, Karl–Heinz Wolf, and Johannes Bruining. Negative Saturation Approach for Non–Isothermal Compositional Two–Phase Flow Simulations. Transport in Porous Media 91(2), 2012.		
RD-04	Hamidreza Salimi, Karl-Heinz Wolf, Johannes Bruining, The influence of capillary pressure on the phase equilibrium of the CO2–water system: Application to carbon sequestration combined with geothermal energy, International Journal of Greenhouse Gas Control, S11, 2012.		
RD-05	Hamidreza Salimi, Karl-Heinz Wolf, Johannes Bruining, The influence of capillary pressure on the phase equilibrium of mixed CO2–water injection into geothermal reservoirs including phase appearance and disappearance. SPE 153886, 2012.		
RD-06	Hamidreza Salimi, Remco Groenenberg, and Karl–Heinz Wolf. Compositional flow simulations of mixed CO_2-water injection into geothermal reservoirs: Geothermal energy combined with CO_2 storage. In: Proc. 36th Workshop on geothermal Reservoir Engineering, Stanford Univ., Stanford, 2011.		
RD-07	Peter Smits, Construction of an integrated reservoir model using the Moerkapelle field for geothermal development of the Delft sandstone, MSc thesis, 2008.		
RD-08	D.T. Gilding, Heterogeneity determination of the Delft subsurface for heat flow modeling, MSc thesis, 2010.		
RD-09	Christian .A. den Boer, The effect of dissolved methane on subsurface flow for heat production from geothermal aquifers, MSc thesis, 2012.		
RD-10	R.C.A. Smit, Optimization of geothermal well doublet placement, MSc thesis, 2012.		

RD-11	Quint de Zeeuw, Modeling two-phase fluid and heat flow in geothermal wells, MSc thesis, 2012.		
RD-12	Tom van den Ende, Mineral Scaling in Geothermal Wells, 2012.		
RD-13	Ruben Logister, Composite versus steel in geothermal wells, 2010.		
RD-14	Steven Leijnse, Friction Coefficient Measurements for Casing While Drilling with Steel and Composite Tubulars, MSc thesis, 2010.		
RD-15	Jonathan Mooij, Exergy analysis of the use of geothermal energy and carbon capture, transportation and storage in Delft Aardwarmte Project, MSc thesis, 2010.		
RD-16	Daniel Reyes Lastiri, Design of a Heating System with Geothermal Energy and CO2 Capture, 2013		

2.3 Abbreviations

(this refers to abbreviations used in this document)

DAP	Delft Aardwarmte Project
DAPP	Delft Aardwarmte Pilot Project
NegSat	Negative Saturation
CwD	Casing while Drilling
HT	High Temperature
MT	Medium Temperature

3 Reservoir characterization

The DAP geothermal wells target the Delft Sandstone Member, a fluvial sandstone formation contained in a structural low at a depths ranging from 1.7 to 2.3 km below surface. The Delft Sandstone Member is deposited in the western and central parts of the West Netherlands Basin. It is a light-grey, fine to coarse-gravelly, massive sandstone sequence with abundant lignitic matter, which varies in thickness between 0 (absent) and 130 m. In order to obtain an economically feasible project the production and injection rate of the geothermal doublet should be approximately 150 m^3 per hour. To achieve this an accurate characterization of the reservoir is essential.

3.1 Construction of an integrated reservoir model using the Moerkapelle field for geothermal development of the Delft sandstone (RD-07)

This work aims to characterize the Delft sandstone; quantify the reservoir properties and uncertainties and analyze the expected flow behaviour for the Delft Geothermal Project. Seismic data, well data and a temperature gradient are integrated in a static reservoir model. From the seismic data an anticline-like structure is determined. The Delft sandstone is part of this structure and it has its top directly below the TU Delft. From the top of the anticline the structure is gently dipping downward in the northeast direction to a depth of about 2150 meters. The structure is bounded by a major fault just southwest of the top of the anticline. The average thickness of the Delft sandstone is expected to be about 56 meters. Due to the sparse regionalized well data for the area around the location of interest for the estimation of the petrophysical properties of the Delft sandstone the Moerkapelle field is used as an analogue. Different scenarios are prepared to evaluate the log data of eight wells of the Moerkapelle field. Depending on the different scenarios the average porosity is between 0.24 and 0.29 and the average permeability is between 290 mD and 970 mD. The probability of reaching the economic production rate of 150 m^3 per hour is estimated to be between 74 % and 79 % for a pessimistic scenario, and between 94 % and 96 % for a positive scenario. The calculated temperature gradient is 3.11 °C per 100 meter, with a surface temperature of 10 ºC. This results in a temperature of 77 °C at a depth of 2150 meters. The major modelling results are described in the next section. The thermal behaviour of the Delft sandstone is modelled in the reservoir simulator STARS, with a 2-D and a 3-D model. The largest effect on the thermal breakthrough is observed when the variation in thickness of the Delft sandstone is applied in the models. The assumed larger thickness at the structural low creates a large accumulation of geothermal energy, causing the reservoir to cool down very slowly. The presence of this structural frame results over 65 years in an insignificant temperature drop at the production well of 1.5 °C. The model results are based on a homogeneous reservoir. To assess the importance of heterogeneity 3-D simulations were run with a high-permeability layer parallel to the flow direction. It creates an earlier thermal breakthrough and a temperature drop of 2°C after 28-30 years. The available data from seismic combined with data from (dry) oil and gas wells is of great use for geothermal projects within the West Netherland Basin.

3.2 Heterogeneity determination of the Delft subsurface for heat flow modeling (RD-08)

In order to study the Co2 co-injection in Delft geothermal aquifer and interference of geothermal projects in the West Netherlands Basin, accurate knowledge of Delft Sandstone Member heterogeneity is necessary. In this study three main goals are considered: 1) gaining a better understanding of the geological setting, the depositional setting and the heterogeneities of the primary target Delft Sandstone Member; (2) demonstrating the effect of heterogeneities in the subsurface on interaction and interference of flow on closely placed geothermal systems; and (3) building a subsurface dynamic reservoir model with which optimal well performance and placement can be assessed.

The basin evolution, depositional setting and depositional processes of the Delft Sandstone Member are determined by combining the available data. The seismic, well, core and cutting data are combined to build a static 3D reservoir architectural model of the Delft subsurface. The static model is incorporated with the flow characteristics from petrophysical log data and used for temperature and fluid flow behavior simulations. By modeling flow and temperature behavior, the flow rates and production temperatures of a single geothermal system and the interference of the different geothermal systems were determined and quantified. This study gives new insights and a better understanding of the reservoir architecture of the Delft Sandstone Member. The Vrijenban Syncline is the predominant structure in the Delft subsurface and the sediments of the Delft Sandstone Member are deposited by a meandering fluvial system in three different depositional settings, controlled by tectonic movement. This has been included in the reservoir model.

The flow simulations in the Delft Sandstone Member show that different geothermal systems closely placed within one reservoir will have pressure interference. Different geothermal systems in one reservoir will however communicate in the reservoir creating both positive and negative effects on flow that are large enough to respectively improve or affect the economics of a project. The results of this study will be a base case for further research, as it will form a benchmark for future local and regional geothermal studies. Simulations of multiple well configurations to determine optimal well placement can now be performed. This will ensure and provide the foundation for a true roll out of geothermal systems through the western parts of the Netherlands.

In this work, several research questions associated with the geothermal wells including: two-phase flow, mineral scaling, and composite material for casing, are addressed.

4 Reservoir modelling

In order to evaluate cold mixed CO_2–water injection into a geothermal reservoir several studies are performed. These include: developing a novel two-phase flow numerical approach; incorporating capillary pressure and gravity, studying the effects of dissolved gas on subsurface flow for heat production, as well as Optimization of geothermal well doublet placement.

4.1 Non-isothermal negative saturation (NegSat) approach (RD-01, RD-03)

We formulate the NegSat solution approach for non-isothermal compositional two-phase flow. Our aim is to have a uniform system of equations for the entire reservoir that could properly deal with different phase states of the reservoir without changing the primary variables and thermodynamic-constraint conditions. For this purpose, we need to know beforehand how many phases could coexist at most. For cold mixed CO_2–water injection into a geothermal reservoir, two phases could coexist at most (viz., a CO_2-rich phase and a water-rich phase). Therefore, we replace the equations for single-phase regions (i.e., oversaturated and undersaturated) with the equations for equivalent fictitious twophase regions with specific properties. We use the principle of equivalence to derive the specific properties. Further details about the non-isothermal NegSat solution approach and non-isothermal compositional multi-phase equations can be found in RD-01, RD-03 and RD-06.

4.2 The Influence of Capillary Pressure on the Phase Equilibrium of the CO_2-Water System: Application to Carbon Sequestration Combined with Geothermal Energy (RD-04, RD-05)

In this work, we include the capillary-pressure effect in the phase-equilibrium calculation of the CO_2-water system. Our rationale to investigate the influence of capillary pressure on the phase equilibrium of the CO_2-water system is that the effect might substantially influence the CO_2-storage capacity and CO_2-trapping mechanism in less permeable zones of reservoirs. Our hypothesis is that inclusion of capillary pressure in VLE reduces the solubility of CO_2 in the aqueous phase and increases the solubility of water in the CO_2-rich (non-wetting) phase. We use thermodynamics to determine the range of capillary pressures for which discernable effects occur in the fluid-phase equilibrium compositions and densities. Subsequently, we quantify the capillary-pressure effect on the CO_2 storage capacity and heat-energy recovery for CO_2-water injection into geothermal reservoirs. Our interest is in the capillary-pressure range between 0 and 100 bars for temperatures between 293 and 372 K and bulk (wetting-phase) pressures between 25 and 255 bars. For this purpose, we have implemented capillary pressure in the PRSV equation of state.

To examine for which values of the injected CO_2 concentrations inclusion of capillary pressure in the phase-equilibrium calculations shows an influence on the displacement process of the CO_2-water system, we simulate mixed CO_2-water injection into a geothermal reservoir. In this way, synergy is established between geothermal-energy production and subsurface CO_2 storage. We apply the non-isothermal negative saturation (NegSat) solution approach to solve efficiently non-isothermal compositional CO_2-water flow that involves phase appearance, phase disappearance, and phase transitions. The advantage of this solution approach is that it circumvents using different equations for single-phase and two-phase regions and the ensuing unstable switching procedure. In this paper, we use the simulation results of mixed CO_2-water injection for various injected CO_2 concentrations to give a complete overview of optimal heat recovery and maximally stored CO_2 for a selected heterogeneity structure derived from the Delft Sandstone Member.

The objectives of this study are (1) to construct a thermodynamic model in which the influence of capillary pressure on the phase equilibrium of the CO_2-water system is included; (2) to quantify conditions for which inclusion of capillary pressure can substantially shift the thermodynamic properties of the CO_2-water system; and (3) to assess inclusion of capillary pressure in the phase equilibrium on the efficiency of CO_2 sequestration and heat-energy recovery for mixed CO_2-water injection into a geothermal reservoir.

The results show that capillary pressure promotes interfacial evaporation. Capillary pressure reduces the CO_2 solubility in water and the aqueous-phase density up to 64% and 1.3%, respectively, whereas it increases the water solubility in the CO_2-rich phase and the CO_2-rich-phase density up to 3,9% (1.0 + 39.5 = 40.5 times) and 1,5%, respectively. Capillary pressure shifts the CO_2 liquid-vapor transition and consequently the upper critical point of the CO_2-water system to a lower pressure. The intensity of the shift depends on the value of the capillary pressure and the bulk pressure.

For mixed CO_2-water injection into a geothermal reservoir, the influence of capillary pressure on the phase equilibrium reduces both the heat recovery and the CO_2-storage capacity up to 37%. We construct a plot of the recuperated heat energy versus the maximally stored CO_2 for a variety of conditions; we compare the results including and excluding the effect of capillary pressure in the phase-equilibrium calculations. We also provide a cursory evaluation of the energy and economics of mixed CO_2-water injection into a geothermal reservoir (see section 6.2).

4.3 The effect of dissolved methane on subsurface flow for heat production from geothermal aquifers (RD-9)

We investigate non-isothermal compositional flow in methane-rich geothermal aquifers by coupling a thermodynamic model and a dynamic flow model. For the thermodynamic model, we develop a MATLAB program, which calculates the thermodynamic equilibrium of the H2OCH4-NaCl mixtures at high-pressure conditions and reservoir temperatures. In the same program we calculate the transport properties. The dynamic flow model is solved using finite element simulations with the NegSat solution approach. We add artificial diffusion and adaptive mesh refinement to obtain a stable solution. Our interest is in the extraction of geothermal energy and our field of study is a reservoir in the Delft Sandstone Member (2200 m depth) and a reservoir in the Main Buntsandstein Subgroup (4000 m depth), both in the West Netherlands Basin. We consider the production of hot methane-rich water and the injection of cold water without methane for both reservoirs.

The objectives of the study are to: 1) determine under which circumstances free methane gas can be present in geothermal reservoirs; 2) quantify how heat recovery is influenced by gas evolution in the reservoir (i.e., the release of solution gas into a free gas phase), and 3) analyze the possibilities for optimal operational conditions for heat recovery and the gas-to-water ratio.

Given the pressure, temperature, salt concentration, thermodynamic equilibrium and gas-water ratio, we can determine the initial phase state of the reservoir and the possibility of gas evolution during production. Solubility and phase density calculations of H2O-CH4-NaCl mixtures are included in the thermodynamic model.

In our simulations, the methane that the reservoirs contain initially is dissolved in the salt water and we investigate cases for different methane concentrations. For high methane concentrations, gas evolution occurs upon the pressure drop at the production well. Using simulation results we show that, even if the initial amount of dissolved methane approaches the solubility limit, the influence of gas evolution on heat extraction is very limited during production and injection. Furthermore, there is no noticeable effect of gas evolution on the water production rate and the production gas-water ratio.
Gas saturations throughout the reservoir remain lower than 0.5% and are too low to alter the heat transfer and to cause upward migration of the evolved solution gas. The low gas saturations have a very low mobility and methane is therefore trapped in the gas phase. As the compositional front of the injected water, with high methane concentration downstream and no methane concentration upstream, progresses into the reservoir, the trapped methane gas will dissolve again in the injected water. Furthermore, the effect of a two-phase region on the relative permeability of water is very low for the conditions studied by us. Near the production well, where an increased pressure drop causes higher

gas saturations (up to 2.2%), water flow rate is only reduced by 0.5-1.8% at maximum and changing operational conditions to optimize the subsurface flow regarding this two-phase flow would not result in noticeable improvements.

4.4 Optimization of geothermal well doublet placement (RD-10)

The lifetime of geothermal projects mainly depends on the thermal breakthrough. Currently, geothermal-energy production is marginally economical because of its uncertainties and risks associated with the subsurface such as lifetime, flow rate, temperature. Lifetime of a geothermal reservoir plays the most important role in the use of geothermal energy because it mainly determines whether or not geothermal-energy production is economically viable.

Through optimization of the well positions from one or more geothermal doublets in a homogeneous or heterogeneous reservoir, the profitability of the project, which is largely dependent on the time of compositional breakthrough, temperature breakthrough and the rate of temperature decline, can be improved. This work studies optimization of the well positions such that the Net Present Value of a project is maximized in a 2D geothermal reservoir for the selected heterogeneity structure. For this purpose an automated, gradient-based optimization method is used. The approach is based on the concept to surround the wells, whose locations have to be optimized, by so-called pseudo-wells. The reservoir simulations are performed using the Finite Element Method in COMSOL Multiphysics. The major features of the simulation results are discussed in detail.

Since the compositional front moves faster than the thermal front, breakthrough of water with altered composition will therefore occur at an early stage in the doublet lifetime. Reservoir heterogeneities influence the time at which thermal and compositional breakthrough occur and also determine the rate at which temperature and composition decline after breakthrough. The temperature and compositional decline curves after breakthrough are generally steeper in a homogeneous reservoir than in a heterogeneous reservoir. Therefore, the thermal breakthrough does not necessarily mean the end of the lifetime of a doublet. It is also shown that the effect of heterogeneities on the thermal retardation factor is small.

Three successful optimization sequences in two different reservoirs are described in this study. It is shown that, from an economical standpoint, it makes little sense to assume a doublet lifetime of more than 30 years. Furthermore, the effectiveness at which a geothermal doublet is able to deplete a reservoir (recovery factor) and profitability of a geothermal doublet are closely interlinked. However, a higher recovery factor does not necessarily mean that the doublet is more profitable and vice versa. There exists an optimum well spacing for doublets positioned in homogeneous reservoirs, such that additional gain of later breakthrough (when placing the production well further away from the injector) is negated by the loss in pressure support of the injection well. This optimum well spacing is found to be an important factor, influencing the profitability in homogeneous and heterogeneous reservoirs.

The heat production from an aquifer can be maximized through the usage of multiple doublet layouts. It is found that, even in a heterogeneous reservoir, it is best to use a checkers-board well arrangement, which is more effective than a tramrail well arrangement.

5 Geothermal wells

In this section, several research questions associated with the geothermal wells including: two-phase flow, mineral scaling, and composite material for casing, are addressed.

5.1 Modeling two-phase fluid and heat flow in geothermal wells (RD-11)

Recently, an amount of methane was produced with hot water in the Ammerlaan geothermal field. The presence of methane influences fluid properties and fluid flow in the well, leading to changes in the pressure and temperature drop in the producing well.

This study presents a model for non-isothermal two-phase flow in geothermal wells. In this model, two-phase flow regimes and their corresponding temperature and pressure drop calculations are coupled. The pressure drop, temperature drop and the flow regime are calculated for different well parameters for the Ammerlaan field. The simulation results are used to give a general overview of optimal well diameter and well inflow rate. Furthermore, the impact of two-phase flow regimes is shown in these simulations.

We found that for a larger well diameter, pressure drop decreases. Pressure drop increases drastically when slug or even churn flow is reached. Smaller well inflow leads to a decrease in pressure drop. Based on the simulation results, the optimal combination of a well diameter of 0,3 meter and well inflow of 40 kg/s are found for the Ammerlaan field.

Besides Ammerlaan, other fields with different salinity and gas contents are investigated in terms of pressure and temperature drop for two-phase flow in a geothermal well. It is found that fields with a low salinity and low gas content are more favorable for geothermal production.

5.2 Mineral Scaling in Geothermal Wells (RD-12)

At the geothermal reservoir hot water with a certain chemical composition is present. The geothermal fluid is brought to the surface by a production well. At the surface the geothermal fluid loses its heat to heat-exchangers. This change in temperature causes the chemical composition of the geothermal fluid to change, which leads to mineral scaling in and clogging of the piping of the system. After the heat extraction the cooled geothermal fluid is re-injected into the reservoir, which induces the warming of the geothermal fluid to reservoir temperature. Again causing the chemical composition to change, leading to potential mineral scaling in and clogging of the geothermal reservoir. Besides the changing temperature during the production and reinjection of the geothermal fluid, degassing and dissolution of gas also have a significant effect on the chemical composition of the geothermal fluid. Therefore, It is necessary in geothermal project to have water treatment, such as chemical treatment or storage of the geothermal fluid in collection tanks for several days to prevent certain minerals from scaling in the reservoir. This can be done, for example, by adding CO_2 to the cooled water to lower pH and preventing possible scaling.

5.3 Composite versus steel in geothermal wells (RD-13)

Two different material, composite and steel, for well casing were exposed to water formation from a geothermal aquifer. The difference in corrosion between steel and composite was clearly visible. Since composite exhibits no typical corrosion, the material is virtually unaffected. Some small changes in the composite are caused by precipitation. But these are so small and will have no adverse effect on the casing. Whereas the corrosion and scaling for the steel sample were significant. Composite appears more resistant than steel to the formation water. It was found that the composite is better suited as a material for casing walls than steel. The reason for choosing steel or composite casing obviously depends on the cost and what effects would be avoided. A combination of steel and composite in a casing would be an option.

5.4 Friction coefficient measurements for casing while drilling with steel and composite tubulars (RD-14)

For the calculation of drilling loads knowledge of the Coulomb friction coefficients for friction between drilling tubulars and casing or drilling tubulars and open hole is essential. To reduce drilling costs for geothermal wells the casing while drilling (CwD) technique is considered. CwD reduces drilling time by eliminating round trips, because the well is drilled and cased simultaneously, thus improving efficiency. Drilling loads are the result of friction in the borehole, the weight of the string, and the borehole and drill string geometries. Drilling costs will be reduced even more if the drilling loads can be reduced. In the Coulomb friction model the ratio between the friction force and the normal force is constant. Thus, if the normal force is reduced, the friction reduces. This can be achieved by replacing the regular heavy steel casing by lighter composite tubulars. Dynamic drilling loads like torsional vibrations can be triggered by the difference in static and dynamic Coulomb friction coefficients. A large difference increases the chance on the occurrence of such friction-induced vibrations. The objective of this study was to compare the Coulomb friction coefficients for steel and composite tubulars, under both static and dynamic conditions, through experiments with the different samples in sand and steel 'boreholes'. If the friction factors for composite casing are known, the dynamic drilling loads for CwD with composite casing can be predicted more accurately. Unfortunately, with the set-up used to measure the dynamic friction coefficients no conclusive results have been obtained. The Coulomb friction coefficients for steel on steel and for steel on “rock" were constant for all applied loads, but the coefficients for composite on steel and for composite on “rock" behaved unexpectedly. In particular, decreasing the normal force seemed to increase the friction coefficients to unrealistically high values. Also the static friction coefficient measurements of the composite casing showed some inconsistencies, which can be contributed to the irregular surface caused by the production process.

6 Exergy analysis

6.1 Exergy analysis of the use of geothermal energy and carbon capture, transportation and storage in Delft Aardwarmte Project (RD-15)

Currently the Delft University of Technology consumes 11 million cubic meters of natural gas to fuel the combined heat and power plant. This causes an emission of 54 tons CO2 every day, 19,740 ton/year. Using geothermal energy as an additional energy source can lower this emission. Assuming that DAPP cover 40% of the heat demands, this would result in preventing 7896 ton/yr CO_2 emission.

Our exergy analysis showed that the amount of energy invested in drilling and materials (steel and cement) is only a minor part of the total energy consumed over the whole lifetime of a geothermal system, including CO_2 co-injection. The largest energy consumption is caused by the capture process, which consumes around 93 % of the total energy input over a 30 years lifetime of the system. In the case of DAP the invested energy and the energy needed to capture 90% of the emitted CO_2 by the combined heat and power plant (running at 60% capacity) is paid back within 4 months, this is of course under ideal conditions.

6.2 Surface heating system with geothermal energy and CO_2 Capture (RD-16)

Heating constitutes about 40% of the final energy consumption at TU Delft. In the present, the district heating system in campus obtains its energy from the combustion of natural gas in a combined heat and power plant. Although this plant produces heat and electricity with an efficiency over 80%, the dependance on a fossil fuel presents an opportunity for improvement by introducing a renewable energy source. In May 2013, the drilling for a geothermal plant in campus was approved.

The present heating system operates at high temperature (HT - 130°C) with 3-way valves. In the new heating system, a geothermal plant will provide part of the energy and some buildings will undergo renovations to work at medium temperature (MT - 70°C); they will be connected in series after HT buildings, constituting a cascade system.

In this study, steady state simulations of the heating system are performed using Cycle-Tempo. The results are then used for an exergy analysis of different configurations in the system.

The analysis of the ongoing transition in the present heating system from a 3-way to a 2-way valve configuration reveals that up to 180 kW of electricity from the grid used for pumping can be saved and replaced by heat produced locally at a higher efficiency, representing up to 36% in primary energy

savings. Within the system boundaries, the exergy efficiency does not improve with the transition, but a reduction in the return temperature from 75-80°C to 50-75°C allows for geothermal energy utilisation. For the new heating system, three configurations of the network are devised: a parallel network at high temperature, a cascade system renovating small buildings and a cascade system renovating large buildings. The exergy analysis reveals that the best option is to renovate the small buildings in campus. In this way, geothermal energy can provide 19% to 50% of the heat demand.
The suggested configuration for the new system can operate with an exergy efficiency 14% higher than the present system, reducing the primary energy consumption and the associated emission of CO_2 by 47%.
Carbon capture and sequestration can decrease the emission of CO_2 further by 51%. However, the capture process by means of the dominant technology, amine absorption, requires additional consumption of fossil fuels, which worsens the scarcity of these resources.

6.3 Exergy analysis of the use of geothermal energy and carbon capture, transportation and storage in Delft Aardwarmte Project (RD-02, RD-07)

Cold mixed CO_2–water injection into geothermal reservoirs can be used to integrate geothermal-energy production and subsurface CO_2 storage. We studied this process in a 2D geothermal reservoir derived from the Delft Sandstone Member below the city Delft (The Netherlands).

The results show that permeability and porosity heterogeneities in a geothermal aquifer significantly influence both heat extraction and CO_2 storage. Hence, reservoir characterization plays an important role in assessing the benefit of CO_2 storage and energy extraction. The CO_2-trapping mechanism is more efficient in the heterogeneous-permeability field because of the larger permeability heterogeneity contrasts and consequently larger capillary effects, compared to the homogeneous-permeability field. In particular, CO_2 banks are mainly formed in the highly permeable zones that are surrounded by less permeable zones. However, the existence of non-isolated highly permeable zones for some injected CO_2 concentrations leads to earlier breakthrough. Moreover, heterogeneity considerably weakens gravity effects. The frequent occurrence of evaporation and condensation, which is particularly effective close to the bubble point, substantially delays CO_2 breakthrough and leads to a larger amount of heat-energy production and CO_2 storage. Based on the simulations, it is possible to construct a plot of the recuperated heat energy versus the maximally stored CO_2 for a variety of conditions.

Fig. 1 plots two curves for the recuperated heat energy versus the maximally stored CO_2 at the end of the process: (1) the curve with the blue-star points excludes the capillary pressure in the phase-equilibrium calculations and (2) the curve with the red-square points includes the capillary pressure in the phase-equilibrium calculations. The figure includes the results for various overall injected CO_2 mole fractions. In Fig. 1, the black-triangular points represent the total energy consumed for each case including the capillary pressure in the phase-equilibrium calculations. For all cases, the initial reservoir conditions, water-injection rate, and injection temperature are the same. However, the overall injected CO_2 mole fraction is different for each case. Along the blue-stars and red- square curves, the overall injected CO_2 mole fraction essentially increases from left to right. With no added CO_2, the criterion to end the project is cold-water breakthrough, while if any amount of CO_2 is added, the criterion to end the project is when CO_2, dissolved into the aqueous phase, breaks through. If the entire pore volume of the reservoir were filled with CO_2 at T = 353.15 K and P = 220 bars, a total CO_2-storage capacity of 13,678 ktonnes would be attained. When no CO_2 were added, a total geothermal-energy production of 16,492 TJ (1 T = 10^{12}) could be achieved.

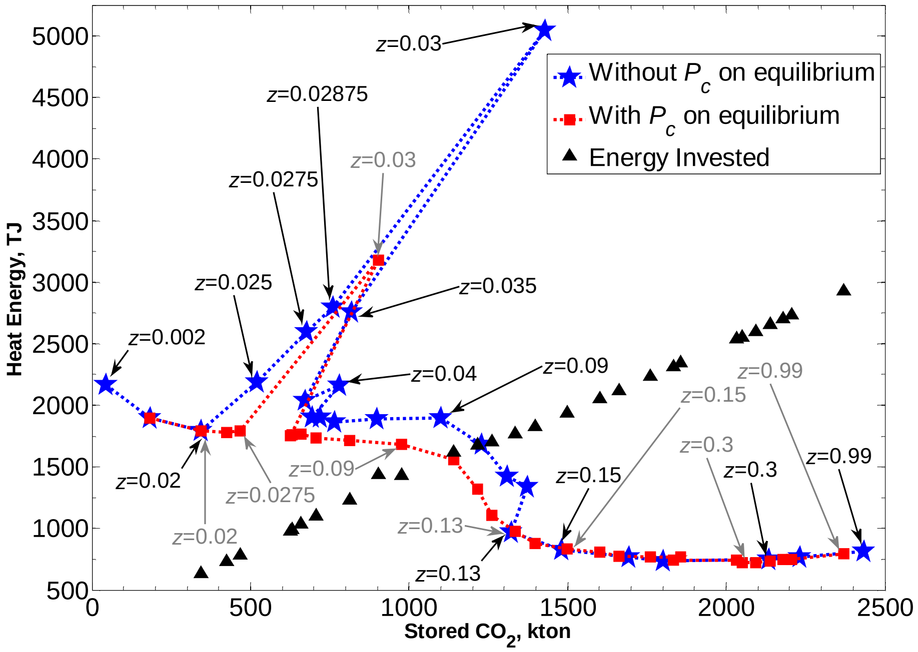

Figure 1—Cumulative heat-energy production and energy invested versus maximally stored CO_2 at the end of the process. We use *z* to denote the overall injected CO_2 mole fraction. The trend from left to right represents an increase in the injected CO_2 mole fraction. The point that corresponds to cold-water injection (i.e., no CO_2) is located on the y-axis (not shown here).